Utah State University
DigitalCommons@USU

International Symposium on Hydraulic Structures

Jan 1st, 12:00 AM - 12:00 AM

Experimental Study of the Influence of Inlet and Outlet Conditions on the Flow Pattern of a Rectangular Shallow Reservoir

Daniel Augusto de Miranda
Federal Institute of Education, Science and Technology of Minas Gerais, IFMG, Santa Luzia, Brazil, d.miranda@ifmg.edu.br

Álefe Marques dos Reis
Methodist University Center Izabela Hendrix, CEUNIH, Belo Horizonte, Brazil, alefe.marques@hotmail.com

Elsa Alves
National Laboratory of Civil Engineering, LNEC, Lisbon, Portugal, ealves@lnec.pt

António Heleno Cardoso
CERIS, Instituto Superior Técnico, IST, Lisbon, Portugal, antonio.cardoso@ist.utl.pt

Márcia Maria Lara Pinto Coelho
Federal University of Minas Gerais, UFMG, Belo Horizonte, Brazil, lara@ehr.ufmg.br

Follow this and additional works at: https://digitalcommons.usu.edu/ishs

Recommended Citation
Miranda, Daniel (2018). Experimental Study of the Influence of Inlet and Outlet Conditions on the Flow Pattern of a Rectangular Shallow Reservoir. Daniel Bung, Blake Tullis, 7th IAHR International Symposium on Hydraulic Structures, Aachen, Germany, 15-18 May. doi: 10.15142/T38063 (978-0-692-13277-7)

This Event is brought to you for free and open access by the Conferences and Events at DigitalCommons@USU. It has been accepted for inclusion in International Symposium on Hydraulic Structures by an authorized administrator of DigitalCommons@USU. For more information, please contact dylan.burns@usu.edu.

UtahStateUniversity
MERRILL-CAZIER LIBRARY

7th International Symposium on Hydraulic Structures Aachen, Germany, 15-18 May 2018
ISBN 978-0-692-13277-7 DOI: 10.15142/T38063

Experimental Study of the Influence of Inlet and Outlet Conditions on the Flow Pattern of a Rectangular Shallow Reservoir

D.A. Miranda[1,4,5], A.M. Reis[2], E. Alves[3], A.H. Cardoso[4] & M.M.L.P. Coelho[5]
[1]*Federal Institute of Education, Science and Technology of Minas Gerais, IFMG, Santa Luzia, Brazil*
[2]*Methodist University Center Izabela Hendrix, CEUNIH, Belo Horizonte, Brazil*
[3]*National Laboratory of Civil Engineering, LNEC, Lisbon, Portugal*
[4]*CERIS, Instituto Superior Técnico, IST, Lisbon, Portugal*
[5]*Federal University of Minas Gerais, UFMG, Belo Horizonte, Brazil*
E-mail: d.miranda@ifmg.edu.br

Abstract: *This article presents an analysis of the influence of symmetrical and asymmetrical positioning of the inlet and outlet channels on flow pattern inside a rectangular shallow reservoir, by means of a series of experiments with clear water in the laboratory. The experimental facility was built in the Hydraulic Research Center (CPH) of the Federal University of Minas Gerais (UFMG), which consisted of a 3 m long and 2 m wide rectangular basin, whose maximum depth was 0.30 m. The inlet and outlet channels were 1.0 m long, 0.125 m wide, and 0.30 m deep. Three different positions were provided for the installation of inlet and outlet channels in their respective transverse walls: left, center, and right. Six different geometric combinations of the inlet and outlet channels were experimentally tested, each under three different flow rates: 0.50, 1.25, and 3.40 l/s. Considering the results related to the unique axis-symmetric configuration, the main jet crossed the basin from upstream to downstream, developing a meander-like path for the lower flow discharge. Moreover, the formation of two large eddies in opposite directions has been noticed, one on each side of the main jet. For the higher flow rates, however, the flow pattern was asymmetrical with the main jet diverting to the right and forming a large counter clockwise vortex. For all the asymmetrical configurations, the flow pattern was also asymmetrical, regardless of the flow rate.*

Keywords: *Shallow reservoirs, sedimentation, flow pattern, physical modeling, geometric configurations, hydrodynamic behavior.*

1. Introduction

Jirka and Uijttewall (2004) defined shallow flows as layered turbulent flows bounded by a bottom surface and by another surface in contact with the atmosphere (free surface), whose horizontal hydraulic characteristics, or their parallel and perpendicular dimensions to the flow, are significantly greater than the vertical one.

The implantation of a shallow reservoir usually leads to the continuous deposition of sediments. Depending on its role, sedimentation must either be maximized (e.g., stabilization ponds in sewage systems) or minimized (e.g., detention basins used for flood control). As highlighted by Dufresne et al. (2010b), the prediction of sediment deposition in such reservoirs is not yet fully understood, as it is a complex function of the geometry of the reservoir, the hydraulic conditions, and the sediment characteristics.

In recent studies, laboratory experiments and numerical simulations have been conducted to better understand, on one hand, the hydraulic behavior and flow patterns associated with rectangular shallow reservoirs, and on the other hand, the sedimentation trends (Jansons and Law 2007; Kantoush 2008; Dewals et al. 2008; Dufresne et al. 2010a,b; Camnasio et al. 2011; Dufresne et al. 2011; Camnasio 2012; Camnasio et al. 2013; Peltier et al. 2015; Peltier et al. 2016; Westhoff et al. 2018; Ferrara et al. 2018).

One of the referenced experimental studies was performed by Dufresne et al. (2010a) in the Laboratory of Engineering Hydraulics of the University of Liège (Belgium). Visual investigation tests were carried out in a 10.40 m long and 0.985 m wide glass flume, using dye injection, which indicated the existence of four flow patterns (as well as an unstable and transitional one), as presented in Fig. 1. These observations were confirmed from Large Scale Particle Image Velocimetry (LSPIV) measurements.

Four flow patterns were identified as a function of their symmetry vs. asymmetry and as a function of the number of circulation zones and location of reattachment points. According to the experimental observations by Dufresne et al. (2010a), flow pattern S0 (Fig. 1a) was observed for comparatively short reservoirs. A straight jet from upstream to downstream, with two symmetrical recirculation zones along either jet sides, characterized this flow pattern.

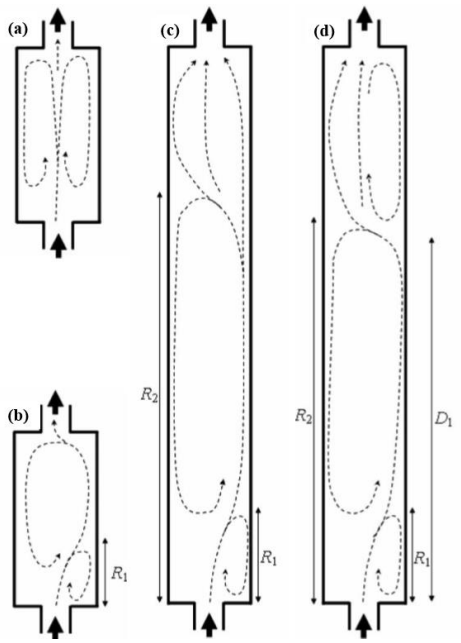

Figure 1. Schematic view of four observed flow patterns: (a) S0, (b) A1, (c) A2, and (d) A3. (Dufresne et al. 2010a) (*adapted*).

If the reservoir length is increased, an asymmetrical flow field can be observed, resulting in flow pattern A1 (Fig. 1b). For intermediate reservoir lengths, a transition flow behavior was reported (A1/S0), oscillating between symmetrical (S0) and asymmetrical (A1) flow patterns (Dufresne et al. 2010a; Camnasio et al. 2011). For longer reservoirs, the experiments revealed an asymmetrical flow field with two reattachment points (A2, Fig. 1c). Finally, for even longer reservoirs, one additional recirculation zone developed in the downstream part of the reservoir (flow pattern A3, Fig. 1d).

In the experimental tests conducted with sediments in symmetrical reservoirs (i.e. inlet and outlet channels located along the reservoir centerline), the flow patterns remained similar to those observed without sediments. The location of the deposits was shown to strongly depend on the flow pattern (Dufresne et al. 2010b). In contrast, Kantoush (2008) noticed that the asymmetrical flow pattern during the clear water tests became almost symmetrical with respect to the centerline of the basin with the addition of sediments.

Camnasio et al. (2013) performed the first experimental and numerical analyses available in the literature considering the influence of asymmetrical locations of the inlet and outlet channels. They observed different stable flow fields depending on the flow history, which highlighted the existence of bi-stable flow fields. In addition, under certain conditions, a completely different flow pattern developed during the tests with sediments compared to the tests with clear water.

The purpose of this paper was to experimentally evaluate the flow patterns observed in a particular shallow rectangular reservoir, taking into account different geometric configurations of upstream and downstream channels positioning and different flow rates.

2. Material and Methods

Laboratory tests have been carried out in the Hydraulic Research Center of the Federal University of Minas Gerais (UFMG, Brazil). A 3.0 m long, 2.0 m wide, and 0.30 m deep rectangular reservoir (Fig. 2) was constructed of sheet metal and covered with epoxy coating in order to protect it against oxidation.

The inlet and outlet channels shown in Fig. 2 were also constructed of sheet metal. Both channels are 1.0 m long, 0.125 m wide, and 0.30 m deep, with the latter corresponding to the same depth of the reservoir. Since the general objective of the research was to evaluate the influence of the positioning of the inlet and outlet channels on the flow pattern, three alternative positions in each transversal wall were provided for the installation of the channels upstream and downstream.

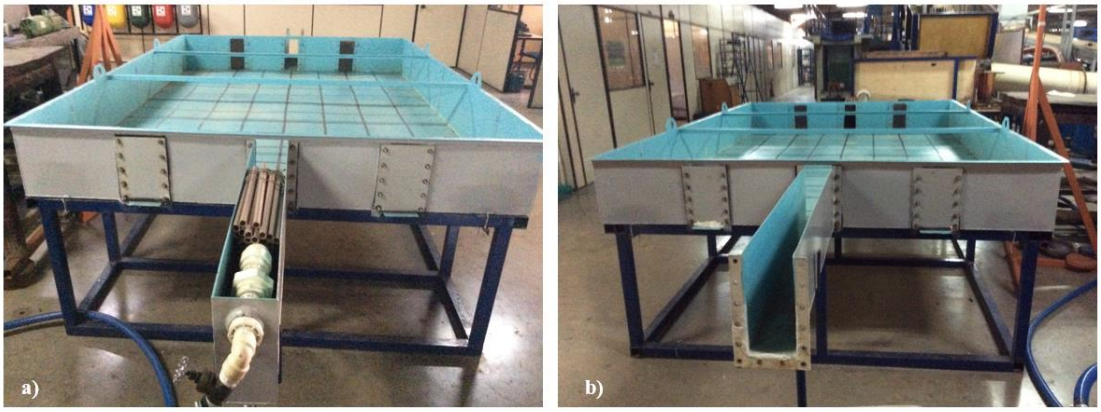

Figure 2. Rectangular reservoir for experiments: (a) inlet channel positioned in the centerline of the basin, (b) outlet channel also positioned in the centerline.

Each of the two channels could be installed with the use of screws in the left position with respect to the flow direction (L-position), in the centerline of the basin (C-position), or finally in the right position (R-position). In order to carry out the clear water experiments, six different geometric combinations of the positioning of the inlet and outlet channels were defined, as presented by Fig. 3. The established settings for the experiments were CC, with upstream and downstream channels installed along the longitudinal axis of the basin (Fig. 3a); LC, with the upstream channel positioned to the left and the downstream channel located to the center (Fig. 3b); LL, with both channels installed to the left in relation to the flow (Fig. 3c); LR, with the upstream channel on the left and the downstream channel on the right (Fig. 3d); RC, with the upstream channel on the right side and the downstream channel on the center (Fig. 3e); and finally CR, based on the installation of the upstream channel along the longitudinal axis of the basin and the downstream channel on the right side (Fig. 3f). In total, 18 tests were carried out, 3 for each geometric configuration and each one for a given flow and its respective water surface level, as shown further in Table 1.

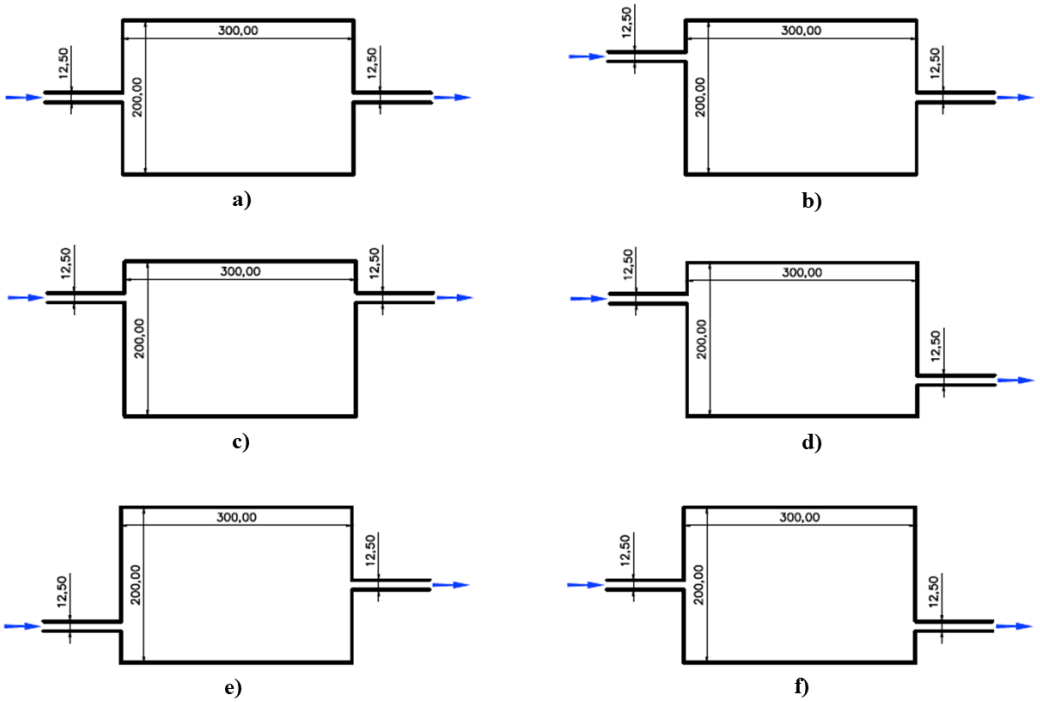

Figure 3. Geometric configurations tested: (a) CC, (b) LC, (c) LL, (d) LR, (e) RC, (f) CR.

It is important to highlight that those geometric configurations were chosen according to the different flow patterns expected to be obtained from all possible combinations between upstream and downstream channels positioning. Nevertheless, two of them were intentionally selected in a redundant way (LC- and RC-configurations) in order to verify if the flow pattern was indeed mirrored.

One of the objectives of the tests carried out in this study consisted of evaluating which of the flow patterns mapped by Kantoush (2008), Dufresne et al. (2010a), and Camnasio et al. (2011) was/were reproduced in the experimental facility constructed in the UFMG laboratory. For this purpose, it was possible to compare the results of the literature, taking into account only the reference condition, related to the installation of the inlet and outlet channels in the centerline of the main basin (CC-configuration). The other configurations have not yet been classified in the literature.

Each geometric configuration was tested with three different flow rates (0.50 l/s, 1.25 l/s, and 3.40 l/s) under steady flow and with clear water. In each test the water depth was measured downstream of the basin, on the initial cross section of the outlet channel, with the aid of a millimeter ruler. In order to control the water level within the rectangular reservoir, a sill with a thickness of 2 mm was installed at the end of the outlet channel and adjusted according to the required water depth. The inlet flow was calibrated during the experiments by means of volumetric measurements and by using a frequency inverter that allowed regulating the rotational speed of the motor-pump assembly.

Table 1 presents the values corresponding to the flows and water depths tested for each geometric configuration.

Table 1. Geometric configurations tested with their respective water depths and flows.

Test number	Geometric Configuration	Water depth H [m]	Q [l/s]
1	CC	0.05	0.50
2		0.10	1.25
3		0.20	3.40
4	LC	0.05	0.50
5		0.10	1.25
6		0.20	3.40
7	LL	0.05	0.50
8		0.10	1.25
9		0.20	3.40
10	LR	0.05	0.50
11		0.10	1.25
12		0.20	3.40
13	RC	0.05	0.50
14		0.10	1.25
15		0.20	3.40
16	CR	0.05	0.50
17		0.10	1.25
18		0.20	3.40

All experiments were filmed (usually during 8 to 12 minutes) for subsequent capture and processing of photos for the determination of surface velocities based on the LSPIV (Large Scale Particle Image Velocimetry) technique. For this purpose, a Logitech webcam C920 model was coupled with a 4.0 m high metallic stand, positioned over the test basin to record high-resolution (HD) videos with up to 1080 pixels. The software FUDAA-LSPIV (Jodeau et al. 2013) has been employed to transform the images into surface velocity vectors. Plastic tracer particles were continuously and uniformly released along the upstream channel during recording.

3. Results and Discussion

3.1. Flow Patterns and Surface Velocities

Table 2 synthesizes the results of all 18 experiments from the same number of figures representing the surface velocity vectors obtained through FUDAA-LSPIV.

Table 2. Distribution of the mean velocity vectors for the 18 experiments performed.

Geometric Config.	Flow rate Q		
	0.50 l/s	1.25 l/s	3.40 l/s
CC	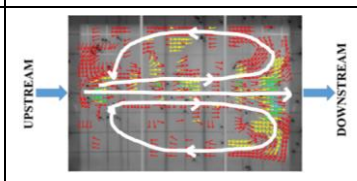	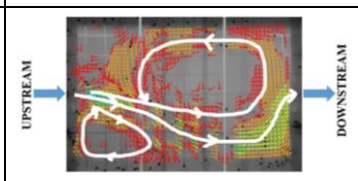	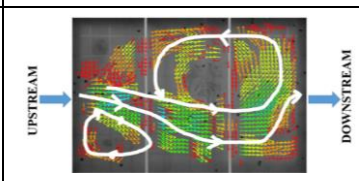
LC	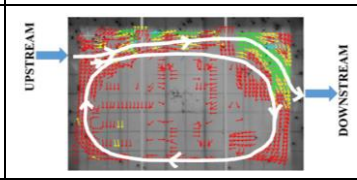	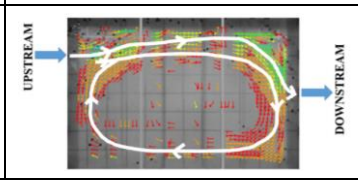	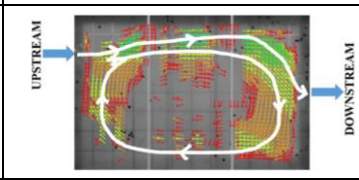
LL	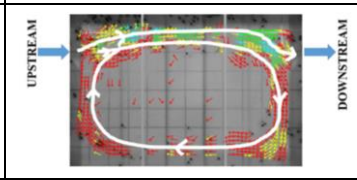	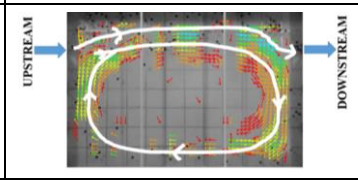	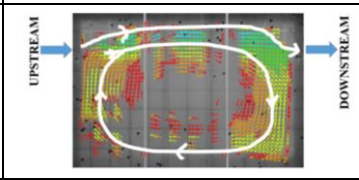
LR	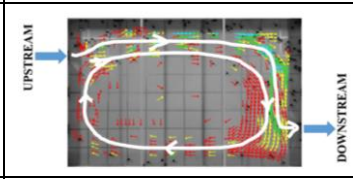	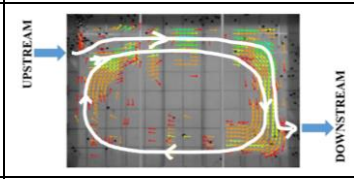	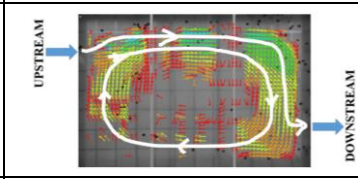
RC	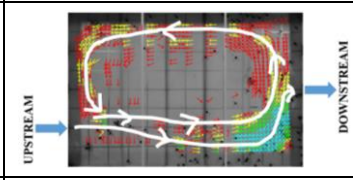	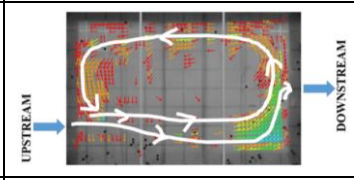	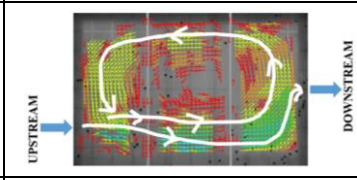
CR	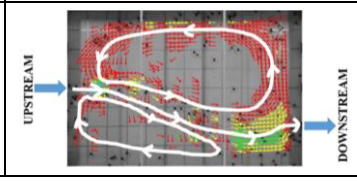	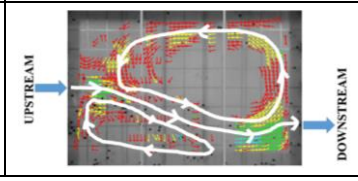	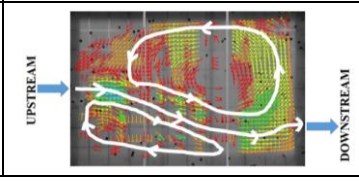

It should be noted that it is only possible to analyze Table 2 in a qualitative way and complement its interpretation with the corresponding values of maximum surface velocities indicated further in Table 3. This table also includes the flow discharge, the upstream channel Froude and Reynolds numbers, the diversion of the main jet, and the direction of rotation of the largest vortex.

With regard to the quality of the flow field results (Table 2), it should be emphasized that it could be significantly improved if a larger amount of plastic tracer particles were used. A uniform distribution of such tracers along the entire upstream wall would also be preferable rather than their insertion only within the upstream channel. This would possibly result in a dense velocity vector mapping.

The flow regime in the final portion of the upstream channel was subcritical in all experiments, with Froude number values between 0.09 and 0.12. In addition, the Reynolds number in the same channel was verified to range between 2100 and 2500 for the flow rate of 0.50 l/s, between 3800 and 4100 for the flow rate of 1.25 l/s, and between 6300 and 7000 for the flow rate of 3.40 l/s. Therefore, these values indicated turbulent flow in all cases. All the obtained values for Froude and Reynolds numbers can be found in Table 3.

Table 3. Main variables observed experimentally in the tests with clear water at UFMG, Brazil.

Geometric Configuration	Q [l/s]	Fr_u*	Re_u**	Diversion of the main jet	Direction of rotation of the largest vortex	Maximum surface velocity [m/s]
CC	0.50	0.10	2365	Nonexistent	-	0.05
	1.25	0.09	4093	Right	Counter-clockwise	0.10
	3.40	0.09	7026	Right	Counter-clockwise	0.14
LC	0.50	0.11	2337	Left	Clockwise	0.05
	1.25	0.10	4101	Left	Clockwise	0.08
	3.40	0.10	6793	Left	Clockwise	0.15
LL	0.50	0.12	2482	Left	Clockwise	0.05
	1.25	0.10	4027	Left	Clockwise	0.09
	3.40	0.10	6819	Left	Clockwise	0.14
LR	0.50	0.10	2302	Left	Clockwise	0.04
	1.25	0.10	3986	Left	Clockwise	0.06
	3.40	0.09	6633	Left	Clockwise	0.14
RC	0.50	0.09	2175	Right	Counter-clockwise	0.03
	1.25	0.09	3796	Right	Counter-clockwise	0.06
	3.40	0.09	6354	Right	Counter-clockwise	0.13
CR	0.50	0.09	2219	Right	Counter-clockwise	0.06
	1.25	0.09	3853	Right	Counter-clockwise	0.06
	3.40	0.09	6309	Right	Counter-clockwise	0.13

*Upstream channel Froude number
**Upstream channel Reynolds number

In relation to the flow pattern characteristic of each experiment, according to Table 2, the flow symmetry condition was observed only for the flow rate of 0.50 l/s of the geometric configuration CC. Moreover, it was noticed that the main jet crossed the basin from upstream to downstream, developing a meander-like path. For the same configuration and discharges Q equal to 1.25 l/s and 3.40 l/s, the observed flow pattern was asymmetrical. Such hydrodynamic asymmetry was observed for all other tests performed, regardless of the flow rate and the positioning of upstream and downstream channels.

It is also important to reiterate that all the experiments were stationary, meaning that the flow remained constant throughout each test. According to Jirka and Uijttewall (2004) and Kolyshkin and Nazarovs (2005), the instabilities identified during the experiments, corresponding to the formation of flow recirculation zones (vorticity), are characteristic of turbulent flows. Therefore, in this aspect, there is a great coherence between the bibliographical references and the hydrodynamic behavior observed in these experiments.

Furthermore, in this study, the shape parameter ($L/\Delta B^{0.60}b^{0.40}$), proposed by Dufresne et al. (2010a) as a combination of dimensionless length ($L/\Delta B$) and lateral expansion ratio ($\Delta B/b$), was 7.16. In this case, the length L of the reservoir was 3.0 m, its lateral expansion width ΔB was equal to 0.938 m, and the length b of the upstream channel was 0.125 m. As pointed out in the studies by Dufresne et al. (2010a), the flow pattern is symmetric if the shape parameter is less than 6.2 and asymmetric if the shape parameter is greater than 6.8. Moreover, there is a transition zone between 6.2 and 6.8 resulting in an unstable flow pattern. In all the tests of those authors, the Froude number was kept constant and equal to 0.20 and the flow was also classified as turbulent. Both parameters were also determined along the upstream channel. Confronting the experimental observations of the present research with the experience of the aforementioned study, there seems to be an incongruence with the results obtained for the flow of 0.50 l/s and a convergence of results for flows of 1.25 l/s and 3.40 l/s. Supposedly, the flow pattern would be asymmetrical for all flows. On the other hand, it should be considered that the established shape parameter was proposed based on high dimensionless flow depths and Froude number equal to 0.20, which is not the case of the study presented here. Dufresne et al. (2010a) also analyzed the influence of the water depth and the Froude number of the hydraulic

conditions. However, the validity limits of the sensitivity analysis of these two parameters are not applicable to the present study.

Kantoush's (2008) experiments were consistent with what was observed in the scope of this study, with only the flow rate of 1.25 l/s being comparable, since the author did not evaluate flows equivalent to those of 0.50 l/s and 3.40 l/s. It is pertinent to mention that the experimental apparatus of the UFMG hydraulic laboratory corresponds, for reasons of convenience for comparison of results, to scale 1:2 of the Kantoush's one. Therefore, the UFMG results, only those related to the CC-configuration, and Kantoush's (2008) experiments have an identical $L/\Delta B$ ratio. The aforementioned author found that there is an asymmetrical flow along the basin characterized by the existence of a large vortex formed from the diversion of the main jet and small vortices in the opposite direction of the larger vortex on the upstream sides of the basin.

When the 18 experiments are analyzed observing the main jet deflection, a direct relationship between this characteristic and the direction of rotation of the largest vortex is verified. The present finding is evident, since this recirculation zone is derived from the main jet deviation and therefore depends on the side at which the deflection of the flow occurs. As previously described by Shapira et al. (1990) and Dewals et al. (2008), the diversion of the main jet is a result of the increase in velocity on one side of this jet, the closest to a side wall, with consequent decrease in local pressure, amplification of flow deflection, and flow asymmetry. This behavior is known as the Coanda effect, which is the main reason for the predominantly observed hydrodynamic instability.

Briefly, the experiments allowed to identify two characteristic behaviors for all hydrodynamically asymmetrical scenarios, as shown in Table 3: (1) when the upstream channel was positioned to the left of the longitudinal axis of the reservoir (L-position), the main jet deviation was always to the left and the larger vortex formed clockwise, regardless of the flow and the positioning of the downstream channel; (2) on the other hand, when the upstream channel was installed in the central position or to the right of the longitudinal axis of the basin (C- and R-positions), the main jet deviation occurred towards the right lateral wall. In addition, the main vortex followed counterclockwise trajectory, except for the 0.50 l/s discharge of the CC-configuration and, in general, regardless of the positioning of the downstream channel.

It is relevant to highlight that, in some experiments, namely those in which the upstream channel was installed in the central position (CC- and CR-configurations), it was possible to identify the formation of a small vortex in the right side of the upstream portion of the reservoir (see Table 2). Its direction of rotation was clockwise, that is, opposite to the main vortex. The only exception was the flow rate of 0.50 l/s for the geometric configuration CC, whose flow pattern is symmetrical.

Concerning the maximum surface velocities identified for each experiment (see Table 3), it does not appear to be a comparable variable among these scenarios, with a view to establishing some kind of influence, per se, on the flow patterns. Therefore, such information is merely illustrative.

3.2. Threshold Between Symmetrical and Asymmetrical Patterns

In order to investigate precisely from which flow rate the flow pattern referring to the geometric configuration CC changes from symmetrical to asymmetrical, three complementary experimental tests were carried out. In this sense, the flow rate was varied in a range between 0.80 l/s and 1.25 l/s, as shown in Table 4, without, however, changing the height of the sill installed in the final section of the downstream channel. That is, an attempt was made to evaluate the sensitivity only of the inflow rate on the flow pattern, despite the small variation of the depth in the reservoir naturally provoked by the variation of the flow discharge.

Table 4. Additional tests referring to the geometric configuration CC for flow rates between 0.80 and 1.25 l/s.

Q [l/s]	d [m]	Fr_u	Flow type	Re_u	Flow type
0.80	0.059	0.14	Subcritical	3659	Turbulent
1.00	0.063	0.16	Subcritical	4428	Turbulent
1.25	0.066	0.19	Subcritical	5406	Turbulent

According to the interpretation of Table 4, there was a gradual increase of the water depth with the increase of the flow rate from one experiment to another, with a difference of 0.7 cm between the flow rates of 0.80 l/s and 1.25 l/s. In all three complementary scenarios, the flow was subcritical (Froude numbers between 0.14 and 0.19) and turbulent (Reynolds numbers between 3659 and 5406). Table 5 summarizes these results.

Furthermore, Table 5 elucidated that the flow pattern remained symmetrical for the flow rate Q = 0.80 l/s, as for the CC-configuration and for the flow rate of 0.50 l/s (Table 2). The only noticeable differences with respect to the flow pattern were a slight increase in the maximum surface velocity (0.05 to 0.06 m/s) with increasing discharge and a slight shortening of the two vortices near the upstream portion of the basin. Concerning the flow rate of 1.00 l/s, the flow pattern remained practically symmetrical even though the vortex to the right of the main jet has not been well represented by the software, probably due to the insufficient quantity of plastic tracer particles used in the experiment. Possibly, it is a transition flow between the two flow patterns, that is, from symmetrical to asymmetrical.

It was also verified that the flow pattern became asymmetrical with increase of the flow rate to 1.25 l/s, with deviation of the main jet to the right side. In addition, the formation of a large vortex in a counterclockwise direction, similar to that observed in Table 2 (CC-configuration, flow rate of 1.25 l/s), but with smaller velocities, no higher than 0.08 m/s against 0.10 m/s of that scenario.

Therefore, it was concluded that the change of the flow pattern from symmetrical to asymmetrical, specifically for CC-configuration, occurred for flow between 1.00 and 1.25 l/s, associated to the water depth of around 6 cm.

Table 5. Distribution of the mean surface velocity vectors for the additional tests (CC-configuration).

Q [l/s]	Mean surface velocity vectors
0.80	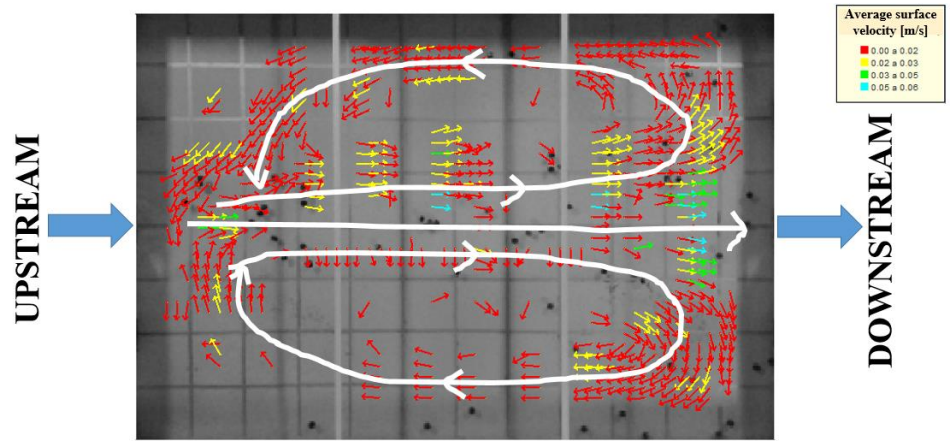
1.00	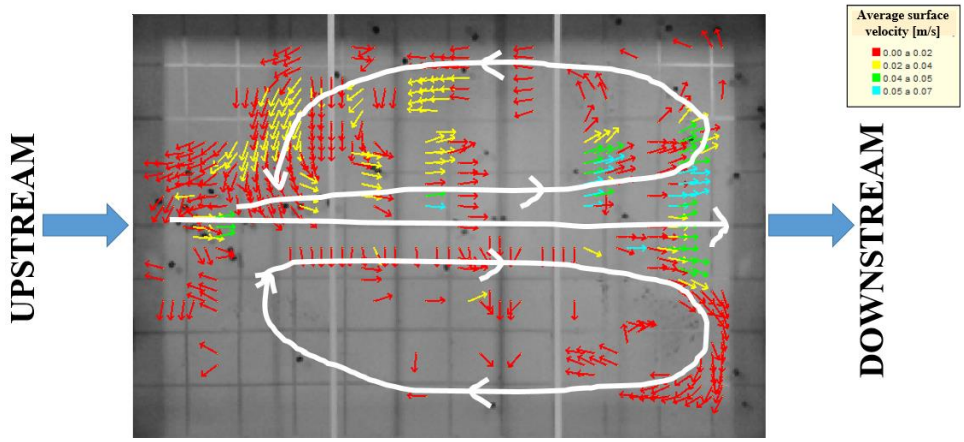

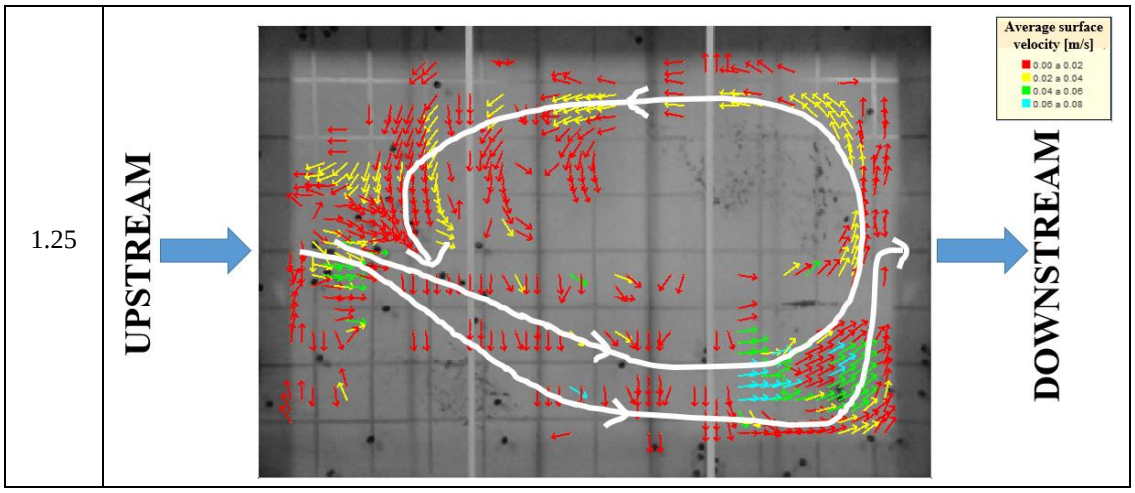

4. Conclusions and Perspectives

Regarding the geometrically symmetrical configuration CC of the reservoir, the experimental tests indicated the existence of hydrodynamic symmetry, corresponding to the development of two vortices of similar proportions and in opposite directions of rotation, for flow rates up to about 1.00 l/s. It was also observed a change on flow pattern from symmetrical to asymmetrical for flow rate between 1.00 and 1.25 l/s. For the larger flows (1.25 l/s and 3.40 l/s), it was observed that the flow pattern was asymmetrical, with the formation of a large anti-clockwise vortex originated from the diversion of the main jet to the right side of the rectangular reservoir.

For the other geometric configurations tested (LC, LL, LR, RC, and CR), it was concluded that the hydrodynamic behavior within the reservoir was also asymmetrical, independent of the flow rate and the positioning of upstream and downstream channels.

In general, concerning the positioning of upstream and downstream channels, it has been noticed that the main jet is diverted to the left if the upstream channel is in the left position and to the right if it is positioned to the center or right positions. It consists of an important perspective to be investigated to physically understand the reason of the "preference" of the main jet to the right side of the basin when the upstream channel is positioned symmetrically with respect to the longitudinal axis of the reservoir. A hypothesis herein formulated may be related to the fact that it would be representative of the hydrodynamic configuration of maximum dissipation in the shear layer between the jet and the recirculation zones, as recently published in the literature by Westhoff et al. (2018). According to the authors, this condition could justify the change from the symmetrical to the asymmetrical flow pattern. However, it seems that their conclusions related to energy dissipation at the interface between the jet and the recirculation zone would not yet be valid for long reservoirs, as is the case of the present study.

Another important aspect to be studied concerns the establishment of a complementary classification of flow patterns for asymmetrical geometries, since the literature has been restricted to symmetrical configurations until now.

In regard to the expected hydrodynamic behavior for the geometric configurations LC and RC, it was verified that the flow pattern in these cases is effectively mirrored. In other words, while for the LC-configuration there is a deviation of the main jet towards the left lateral wall, resulting in the formation of a large vortex clockwise, for the RC-configuration, the behavior is similar, however, with inverted senses.

5. Acknowledgements

The authors acknowledge the Brazilian National Council for Scientific and Technological Development (CNPq) for providing funding for the assembly of the experimental apparatus and acquisition of support materials used during the laboratory experiments. The authors would also like to thank Prof. Benjamin J. Dewals of the University of Liège (ULg, Belgium) for his collaboration and suggestions for this research. Moreover, the first author acknowledges the Federal Institute of Education, Science and Technology of Minas Gerais (IFMG Campus Santa Luzia, Brazil) for its

collaboration with this work and, in particular, the Portuguese Foundation for Science and Technology (FCT) for financial support during his permanence in Portugal, through its funding program PD/BD/135219/2017. Finally, the authors would like to express their sincere thanks to the two reviewers who provided extremely relevant contributions to the improvement of the manuscript.

6. References

Camnasio, E., Orsi, E., and Schleiss, A. (2011). "Experimental study of velocity fields in rectangular shallow reservoirs." *J. Hydraul. Res.,* 49(3), 352-358.

Camnasio, E. (2012). "Investigation of flow patterns and sedimentation in rectangular shallow reservoirs." *PhD Thesis*. Politecnico di Milano.

Camnasio, E., Erpicum, S., Orsi, E., Pirotton, M., Schleiss, A., and Dewals, B.J. (2013). "Coupling between flow and sediment deposition in rectangular shallow reservoirs." *J. Hydraul. Res.,* 51(5), 535-547.

Dewals, B.J., Kantoush, S.A., Erpicum, S., Pirotton, M., and Schleiss, A.J. (2008). "Experimental and numerical analysis of flow instabilities in rectangular shallow basins." *Environ. Fluid Mech.,* 8(1), 31–54.

Dufresne, M., Dewals, B.J., Erpicum, S., Archambeau, P., and Pirotton, M. (2010a). "Classification of flow patterns in rectangular shallow reservoirs." *J. Hydraul. Res.,* 48(2), 197-204.

Dufresne, M., Dewals, B.J., Erpicum, S., Archambeau, P., and Pirotton, M. (2010b). "Experimental investigation of flow patterns and sediment deposition in rectangular shallow reservoirs." *Int. J. Sediment Res.,* 25(3), 258-270.

Dufresne, M., Dewals, B.J., Erpicum, S., Archambeau, P., and Pirotton, M. (2011). "Numerical investigation of flow patterns in rectangular shallow reservoirs." *Eng. Appl. Comp. Fluid Mech.,* 5(2), 247-258.

Ferrara V., Erpicum, S., Archambeau, P., Pirotton, M., and Dewals, B.J. (2018). "Flow field in shallow reservoir with varying inlet and outlet position." *Journal of Hydraulic Research*., DOI: 10.1080/00221686.2017.1399937.

Jansons, K., and Law, S. (2007). "The hydraulic efficiency of simple stormwater ponds." *13th International Rainwater Catchment Systems Conference*, Sydney, Australia, August 2007.

Jirka, G.H., and Uijttewaal, W.S.J. (2004). "Shallow flows: a definition." Jirka, G.H., Uijttewaal, W.S.J. (Eds.), Proc. *Shallow Flows*. Balkema publ., 2004. ISBN: 90 5809 7005.

Jodeau, M., Hauet, A., and Le Coz, J. (2013). "Fudaa-LSPIV 1.3.2—Guide d'utilisation." *EDF R&D, EDF DTG, Irstea*, < https://forge.irstea.fr/projects/fudaa-lspiv/files> (Nov.10, 2017).

Kantoush, S.A. (2008). "Experimental study on the influence of the geometry of shallow reservoirs on flow patterns and sedimentation by suspended sediments." EPFL, Lausanne, Switzerland, *PhD thesis* 4048.

Kolyshkin, A., and Nazarovs, S. (2005). "On the stability of wake flows in shallow water." *Abstracts of 10th International Conference on Mathematical Modelling and Analysis*. Matematikos ir Informatikos Institutas, 83.

Peltier, Y., Erpicum, S., Archambeau, P., Pirotton, M., and Dewals, B. (2015). "Can meandering flows in shallow rectangular reservoir be modelled with the 2D shallow water equations?" *Journal of Hydraulic Engineering*, ASCE, 141(6), 1-10.

Peltier, Y., Erpicum, S., Archambeau, P., Pirotton, M., and Dewals, B. (2016). "Numerical modelling of meandering jets in shallow rectangular reservoir using two different turbulent closures." *IAHR Europe Congress*, Liège, Belgium, 2016.

Shapira, M., Degani, D., and Weihs, D. (1990). "Stability and existence of multiple solutions for viscous flow in suddenly enlarged channels." *Comput Fluids*, 18(3), 239-258.

Westhoff, M.C., Erpicum, S., Archambeau, P., Pirotton, M., and Dewals, B. (2018). "Maximum energy dissipation to explain velocity fields in shallow reservoirs." *Journal of Hydraulic Research*. 56(2), 221-230.